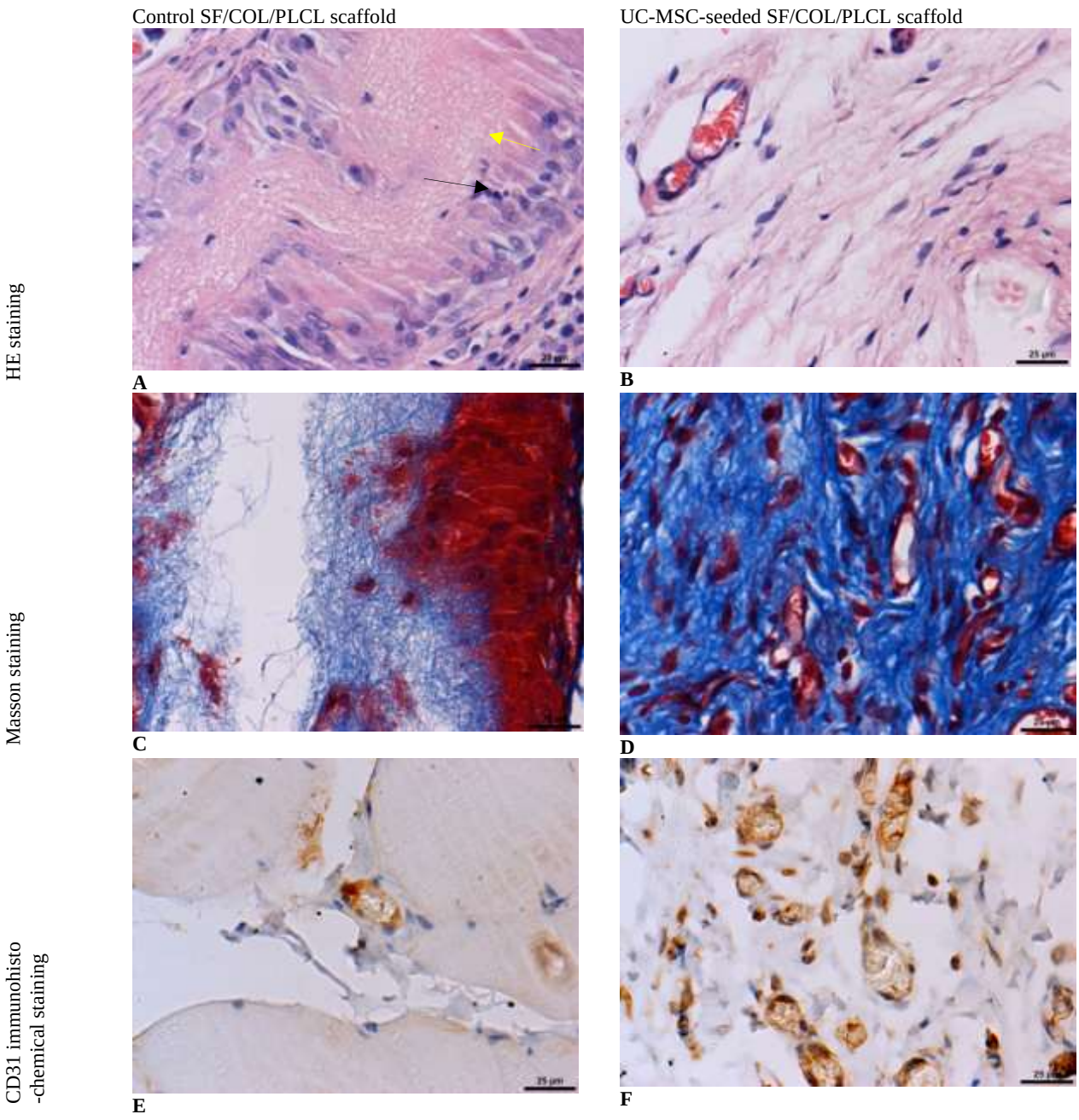

Biocompatibility of MSC-Seeded Pelvic Patch

New Medical Innovations and Research

Authored by

Jin Keqin [1#], Luo Jianfeng [1,2*#], Su Aifang [1], Ding Mingxing [3], Fu Saihong [1] and Fang Yuanshu [4]

[1]Genetic Laboratory, Jinhua Maternal & Child Health Care Hospital, Jinhua, 321000, Zhejiang Province, China.

[2]Central Laboratory, Affiliated Jinhua Hospital, Zhejiang University School of Medicine, Jinhua, 321000, Zhejiang Province, China.

[3]Medical Molecular Biology Laboratory, School of Medicine, Jinhua Polytechnic, Jinhua 321007, China.

[4]Jinhua Center of Laboratory Animals, Jinhua Municipal Food and Drug Inspection Institute, Jinhua, 321000, Zhejiang Province, China.

Published Date

August 02, 2022

Published in the Journal of

New Medical Innovations and Research

Auctores Publishing, LLC

16192 Coastal Highway

Lewes, DE 19958,

United States of America

AUCTORES
Globalize your Research

New Medical Innovations and Research

Luo Jianfeng *

Open Access

Research Article

Biocompatibility of MSC-Seeded Pelvic Patch

Jin Keqin [1#], Luo Jianfeng [1,2*#], Su Aifang [1], Ding Mingxing [3], Fu Saihong [1] and Fang Yuanshu [4]

[1] Genetic Laboratory, Jinhua Maternal & Child Health Care Hospital, Jinhua, 321000, Zhejiang Province, China.

[2] Central Laboratory, Affiliated Jinhua Hospital, Zhejiang University School of Medicine, Jinhua, 321000, Zhejiang Province, China.

[3] Medical Molecular Biology Laboratory, School of Medicine, Jinhua Polytechnic, Jinhua 321007, China.

[4] Jinhua Center of Laboratory Animals, Jinhua Municipal Food and Drug Inspection Institute, Jinhua, 321000, Zhejiang Province, China.

***Corresponding Author:** Luo Jianfeng, Central laboratory, Affiliated Jinhua Hospital, Zhejiang University School of Medicine, No. 365 Renmin East Road, Jinhua, 321000, Zhejiang Province, China.

# Equally contributed to this work

Received date: July 12, 2022; Accepted date: July 25, 2022; Published date: August 02, 2022

Citation: Jin Keqin, Luo Jianfeng, Su Aifang, Ding Mingxing, Fu Saihong, et al. (2022). Biocompatibility of MSC-Seeded Pelvic Patch. *J New Medical Innovations and Research*, 3(1); DOI:10.31579/2767-7370/028

Abstract:

Objective: To investigate the Biocompatibility of a silk fibroin/collagen/poly (lactide-co-caprolactone) (SF/COL/PLCL) electrospun three-dimensional nanofibre scaffold seeded with human umbilical cord-derived mesenchymal stem cells (UC-MSCs) in rats.

Methods: Twelve adult male Sprague-Dawley rats were randomly divided into two groups of six; the first received a patch seeded with UC-MSCs, whereas the second received a control patch without UC-MSCs. The patches were implanted subcutaneously in the abdomens of rats, and subsequent inflammatory reactions and levels of tissue generation and angiogenesis were monitored over a 12-week period using haematoxylin-eosin and Masson staining, alongside quantitative fluorescence PCR.

Results: The cell viability was strongest when the SF/COL/PLCL patch was seeded with UC-MSCs for up to 7 days, and cells retained normal morphology and structure when viewed under an electron microscope. The implanted patches seeded with UC-MSCs showed better tissue fusion, faster degradation, and higher deposition of collagen fibres and neovascularization than the naked patches for up to 12 weeks, ($p<0.01$), but there was no significant difference in fibrosis scores between the two groups ($p>0.05$). By the end of the study, rats receiving the seeded nanofibre implants showed improved inflammation resolution, as reflected by lower IL-6 levels ($p<0.01$). However, IL-2, IL-8, and TNF-α levels were not significantly different between the two groups ($p>0.05$).

Conclusion(s): The application of UC-MSCs to SF/COL/PLCL patches has the potential to improve the levels of tissue fusion and reduce inflammation, making it a potential treatment for human pelvic floor reconstruction.

Keywords: inflammatory response; pelvic patch; SF/COL/PLCL; UC-MSC; FPFD

1. Introduction

Female pelvic floor dysfunction (FPFD) is a common problem faced by middle-aged and older women, with an estimated burden of morbidity between 30 and 50% [1,2]. This condition can lead to anatomical and structural changes to the reproductive and surrounding organs, resulting in abnormalities in their position and function, and eventually presenting as a pelvic organ prolapse (POP) and stress urinary incontinence. Although the disease does not pose a threat to the life of the patient, it impacts their quality of life and as a consequence, results in a psychological burden.

Pelvic floor reconstruction is an important treatment for FPFD and accounts for 40–60% of general gynaecological surgery. The complexity of the pelvic floor structure and its mechanics, with mean disease recurrence rates up to 19%, can often necessitate the need for reoperation [3]. In recent years, owing to the emergence of new surgical techniques, both synthetic and biomaterial patches have been increasingly used in clinical settings; however, these materials have their own pros and cons [4,5]. Complications of using these patches include vaginal erosion, recurring infections, granuloma, dyspareunia, vesicovaginal fistula, and chronic pain. In July 2011, the Food and Drug Administration issued a second warning on the use of non-absorbable scaffold polypropylene

patches in FPFD surgery, based on the potential of these patches to cause infections, graft-versus-host disease, and persistent postoperative pain [6,7]. Patches made from biomaterials reduce several of the complications associated with the use of foreign materials, but their clinical application is limited by poor efficacy; hence, there is a need for better treatment options.

A new approach to treating FPFD is use of a biological substitute composed of seed cells cultured *in vitro*, along with scaffold materials. These biological substitutes have the ability to repair the damaged parts of human tissue and organs because as the scaffold materials degrade, the seed cells proliferate, differentiate, and form new tissues, facilitating wound repair and ultimately functional reconstruction [8]. The success of biological substitutes depends on two aspects: the choice of seed cells and the scaffold materials used.

Mesenchymal stem cells (MSCs) are multipotent adult stem cells present in multiple tissues, including umbilical cord, bone marrow, and fat tissue; they can self-renew by dividing and can differentiate into multiple tissues [9,10]. Bone marrow mesenchymal stem cells (BMSCs) were among the first MSCs to be characterized and used in the regenerative medicine clinical setting; however, the process of bone marrow extraction is not readily accepted by patients, and this limits their potential application in PFD. In contrast, human umbilical cord-derived mesenchymal stem cells (UC-MSCs) have similar properties to BMSCs, with the added advantage that they can be more easily sourced, have higher amplification capacities, and carry a lower risk of bacterial/viral infections; moreover, the chance of rejection graft-versus-host disease is lower. Previous reports [11] have demonstrated that UC-MSCs can induce tissue-forming cells in mice, confirming their potential to play a role in fascia tissue engineering. Ding *et al*. recently developed a few candidate nanofibrous materials suitable for pelvic reconstruction, which showed high UC-MSCs adhesion capacity. These developments suggest that UC-MSCs would be an ideal seed cell source for female pelvic floor reconstruction.

In terms of scaffolding, nanocomposite materials offer advantages over simple scaffold materials [12,14], because they can simulate the extracellular matrix microenvironment in ways similar to human tissue. For example, collagen (COL) can directly or indirectly influence the process of cell proliferation, adhesion, and differentiation [15]. Further, poly(L-lactide) can easily be degraded in 30–50 weeks [16] and polyester–polycaprolactone has excellent biocompatibility and mechanical properties [17].

To date, only a few studies have investigated the integration of MSCs and bio-degradable nano-filament membranes and the overall graft-versus-host reaction to them [18,19]; therefore, little is known about how stem cells combined with nano-fibrous materials could improve pelvic floor reconstruction outcomes. Despite ongoing research in the field of cell-based tissue engineering, it is still unclear how the reticular structures of the nanocomposites affect stem/progenitor cells and ultimately long-term tissue integration. In this study, we investigate the Biocompatibility of a silk fibroin/collagen/poly(lactide-co-caprolactone) (SF/COL/PLCL) electrospun three-dimensional nanofibre scaffold seeded with human umbilical cord-derived mesenchymal stem cells (UC-MSCs) in rats. The findings of this study could form the basis of future mesh applications in female pelvic floor reconstruction.

2. Materials and Methods

2.1. hUC-MSC transfection with a GFP-carrying lentivirus

The isolated UC-MSCs cells were cultured and amplified in 24-well plates. In total, 3.5×10^4 cells were added to each well and incubated overnight. The fluid was replaced when the cell coverage rate reached 60%. Virus amounts, corresponding to different MOI values, were added. The medium was changed after 8 hours of viral infection, then cells were cultivated for an additional 48 hours. When the viral particle titre reached 1×10^8 TU/ml, the cells were collected for subsequent experiments [20].

2.2. Manufacture of electrospun three-dimensional nanofiber scaffold

SF/COL/PLCL electrospun three-dimensional nanofibre scaffolds were manufactured as follows: SF, COL, and PLCL were dissolved in hexafluoroisopropanol solution in the mass ratio of 7:3:10, according to Liu et al [21]. The polymer solution (8%) was electrospun at a voltage of 11 kV, achieving a distance of 12 cm and ejection velocity of 1.5 ml/h. The scaffold was then desiccated in a vacuum drying chamber.

2.3. Detection of the growth and proliferation of UC-MSCs on the nanofibre

The lentivirus-transduced cells were inoculated onto the three-dimensional nanofibre scaffold. Cell morphology was observed by a scanning electron microscope on days 5, 7, and 9 after inoculation. Finally, the CCK8 assay was used to determine the cell proliferation state.

2.4. Implantation of nanofibre scaffolds

Twelve SD rats, purchased at 4 weeks of age, were randomly divided into two groups. After being anesthetised with 10% chloral hydrate (300 mg/kg), the rats were fixed in a supine position and a 1 cm long incision was made in the lateral ventral wall. The SF/COL/PLCL mesh loaded with UC-MSCs was implanted subcutaneously in the abdomen of rats in the experimental group. A simple SF/COL/PLCL mesh was implanted subcutaneously in the abdomen of the rats in the control group. The survival and distribution of the transplanted cells was observed at 1, 4, and 12 weeks post-implantation. The rats were euthanised, and the mesh was retrieved. The inflammatory reaction, tissue generation and angiogenesis, fibre wrapping, and scaffold degradation of the two groups were compared using haematoxylin-eosin and Masson staining. The levels of inflammatory cytokines, specifically IL-2, IL-6, IL-8, and TNF-α, in the tissue surrounding the implanted scaffold were measured using quantitative fluorescence PCR.

2.5. Histopathological observations following implantation

The tissue samples were immediately immobilised in a 4% paraformaldehyde solution and dehydrated with ethanol for paraffin sectioning (4–5 μm). The inflammatory cell infiltration was observed, according to standard haematoxylin and eosin staining, Masson staining was used to detect fibrosis, and CD31 immunohistochemical labelling was used to detect new blood vessels. The tissue samples, collected at the different time points, were examined semi-quantitatively under a light microscope. Individual slides were scored from 0–4 (0: none, 1: minimum, 2: mild, 3: intermediate, 4: severe), in terms of inflammatory cell infiltration, the level of fibration, and angiogenesis [22].

2.6. Quantitative analysis of IL-2, IL-6, IL-8, and TNF-α with qRT-PCR

Total RNA was extracted from cells using TRIzol reagent, according to the manufacturer's instructions. *IL-2*, *IL-6*, *IL-8*, *TNF-α*, and *β-actin* products were amplified by qRT-PCR, using *β-actin* as the internal reference. The conditions of qRT-PCR amplification were as follows: 95°C for 30 seconds, 95°C for 10 seconds, and then 40 cycles at 60°C for 30 seconds. The specific primer sets used to detect gene mRNA expression are shown in Table 1. The comparative threshold (Ct) method was used to determine the amount of target gene mRNA, by normalising the target mRNA Ct value to the GAPDH value (ΔCt).

Table 1: *Specifications of primer sequences used for quantitative real-time PCR*

Species	RNA name	Primer type	Primer sequence
Rat	IL-2	F	TCCCCATGATGCTCACGTTT
Rat	IL-2	R	TCCGAGTTCATTTTCCAGGCA
Rat	IL-6	F	AGCGATGATGCACTGTCAGA
Rat	IL-6	R	GGAACTCCAGAAGACCAGAGC
Rat	IL-8	F	ACTGAGCCCCTCCCTACTAA
Rat	IL-8	R	TGTCTTCAATCCATCCCAGAGC
Rat	TNF-α	F	AAGGAGGAGAAGTTCCCAAATG
Rat	TNF-α	R	GGGCTACGGGCTTGTCACTC
Rat	β-actin	F	CCCATCTATGAGGGTTACGC
Rat	β-actin	R	TTTAATGTCACGCACGATTTC

3. Statistical analysis

Statistical analysis was performed using SPSS 23.0 software (IBM Corp., Armonk, NY, USA). Quantitative data are expressed as the mean ± standard deviation. Between-group comparisons were performed using repeated measures ANOVA followed by Tukey's honestly significant difference (HSD) test. Qualitative data were expressed as the rate, and within-group comparisons were made using the Chi-squared test. $p<0.05$ was considered to imply statistically significant differences.

4. Results

4.1. Cell growth and proliferation after nanofibrous scaffold implantation

Lentiviral transduction did not adversely affect cell viability. Cell viability increased significantly after 5 days of inoculation and continued to increase until day 7 but declined from day 9 onwards. The survival rate of the cells at different time periods following implantation showed statistical significance (F=702.85, $p<0.01$; Figure 1).

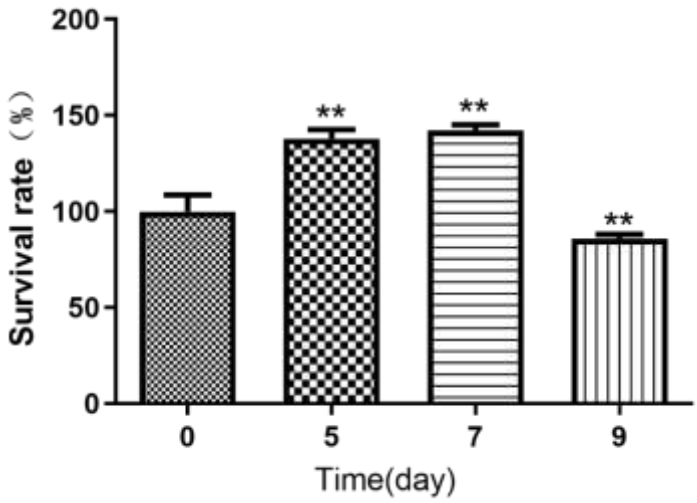

Figure 1: *The time course of umbilical cord-derived mesenchymal stem cell (UC-MSC) survival rate on nano-fibrous scaffolds post-implantation. *p<0.05, **p<0.01*

4.2. Cell morphology of lentivirus-transfected UC-MSCs post-implantation on nano-fibrous scaffolds

The cellular morphology was normal on day 7, and the cells showed a normal structure with strong extensions and a significant increase in proliferation ability. By day 9, the cellular proliferation ability had decreased, and the cells showed swelling and structural disconnections (Figure 2).

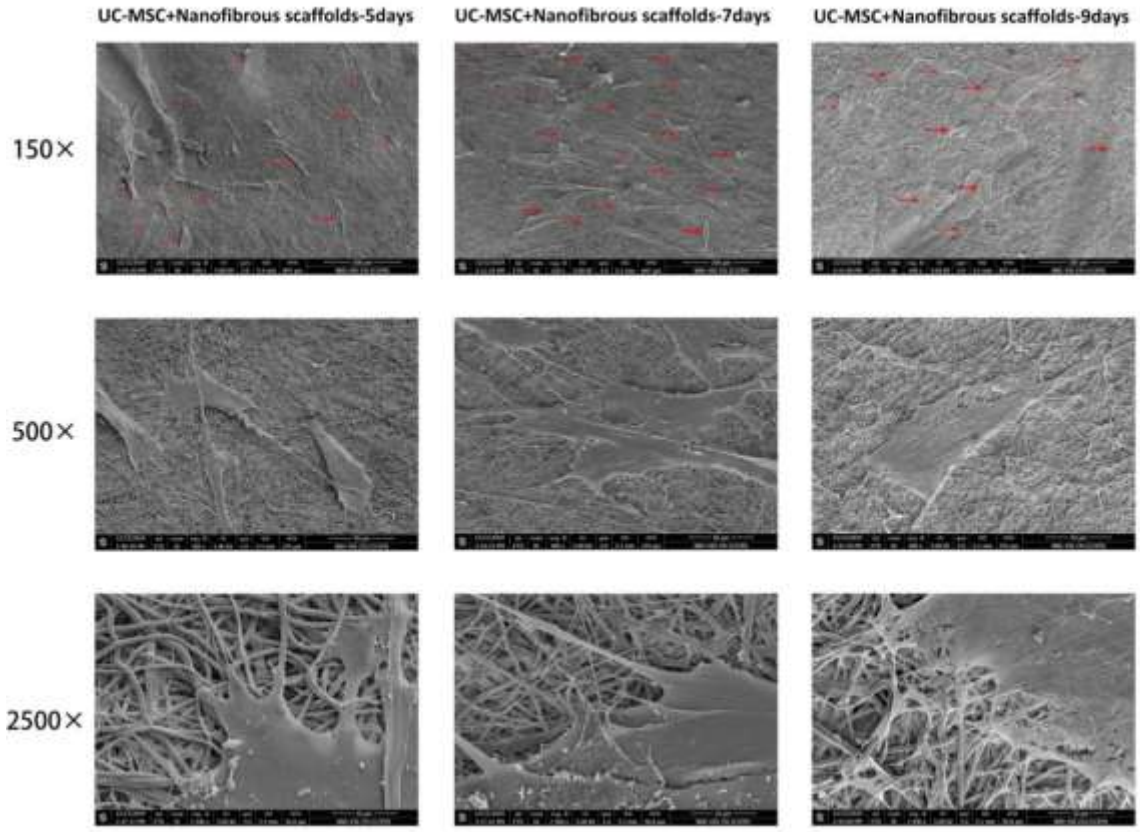

Figure 2: *Scanning electron microscope images showing cell morphology of umbilical cord-derived mesenchymal stem cells (UC-MSCs) at different time points post-implantation onto the nano-fibrous scaffolds. The red arrows, identified based on the lowest magnification images (150×, scale bar = 200 μm), identify the cells, shown at high magnification levels (500×, scale bar = 50 μm and 2500×, scale bar = 10 μm).*

4.3. Histopathology assessment

The H&E staining revealed that the SF/COL/PLCL control group showed a clear scaffold structure at week 1 and 4. The scaffold slowly degraded as time passed, and by week 12, the scaffold's central area was no longer visible and the surrounding tissues had covered the peripheral area. In the UC-MSC-seeded scaffold group, the nano-fibrous membrane was still intact at week 1, but there had been significant infiltration by inflammatory cells. The scaffold structure was completely disintegrated by week 4, and by week 12, the inflammatory cell infiltration had subsided. The level of inflammatory cell infiltration was significantly different between the control SF/COL/PLCL nano-fibrous membrane and the UC-MSC-seeded nano-fibrous membrane groups ($F=23.79$, $p<0.01$) (Figure 3, 4).

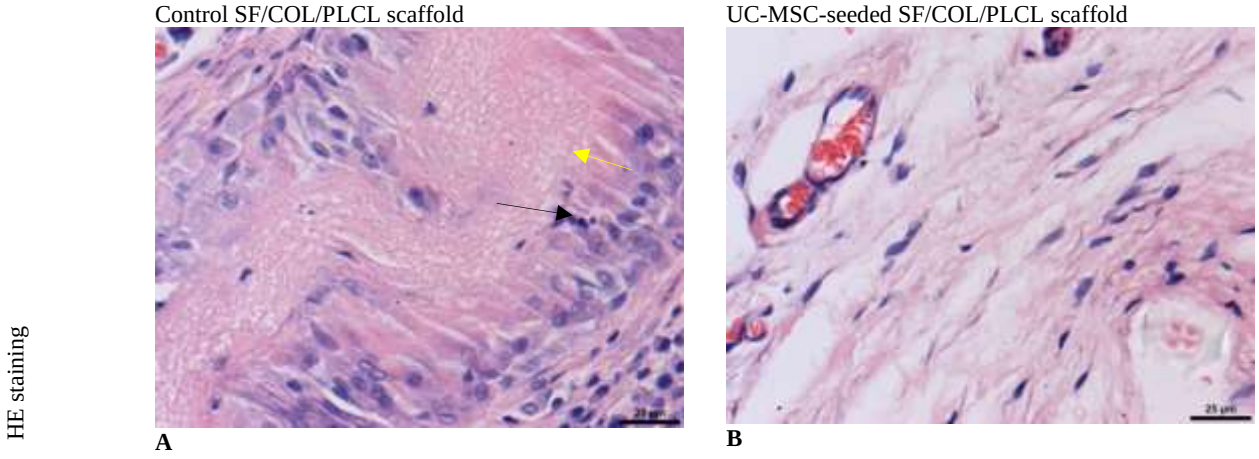

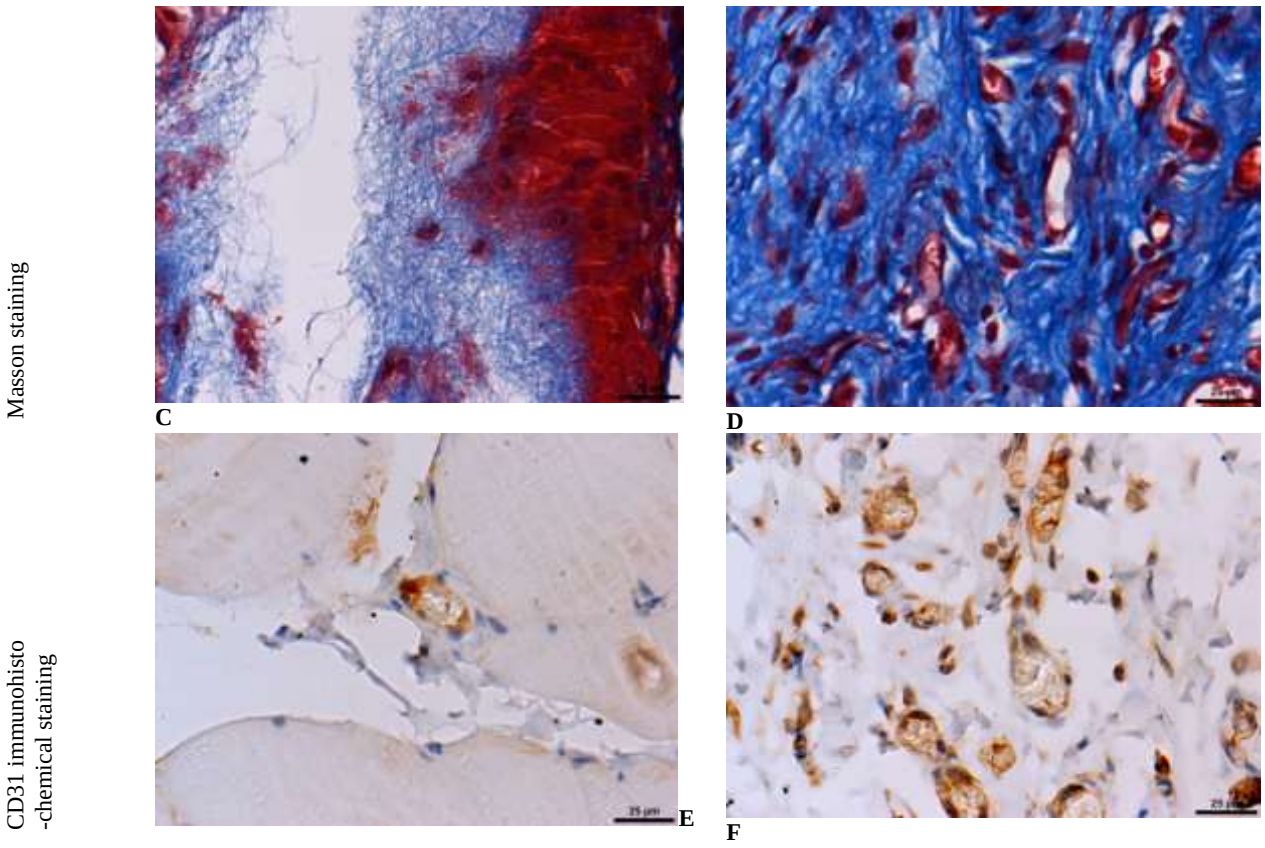

Figure 3: *Pathohistological analysis of the naked and umbilical cord-derived mesenchymal stem cell (UC-MSC)-seeded silk fibroin/collagen/poly(lactide-co-caprolactone) (SF/COL/PLCL) nano-membrane (Scale bar, 25 μm). A,B,H&E staining: showing the Cell Nucleus in blue/purple-blue, the cytoplasm in pink, and RBCs in bright red. The black arrow shows inflammatory cell infiltration, and the yellow arrow marks the position of the scaffold. C,D, Masson staining: cells are shown in red, collagen fibres in blue, and nuclei in cyanotic blue. E,F, CD31 immunohistochemistry staining: recently synthesised blood vessels with CD31 stain brown or yellowish-brown.*

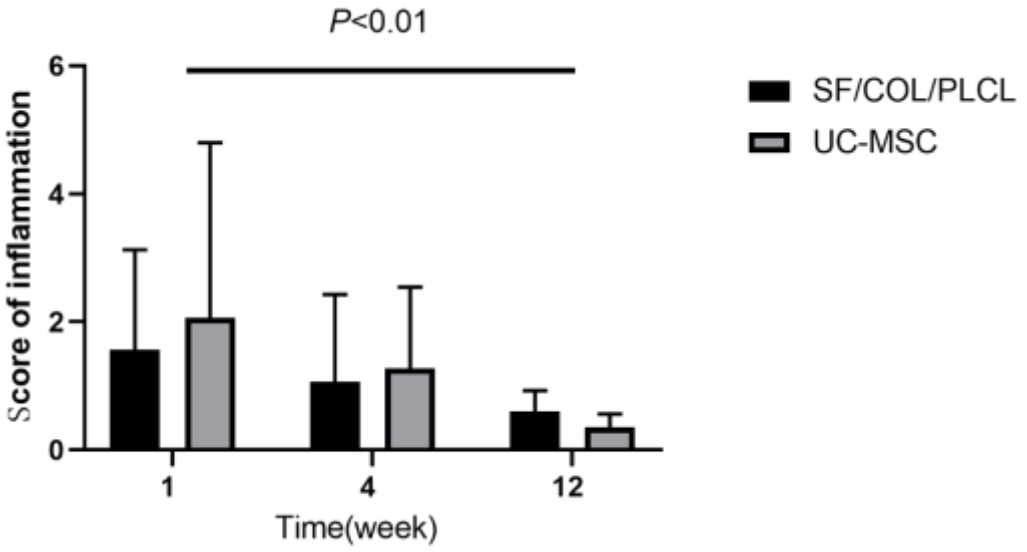

A

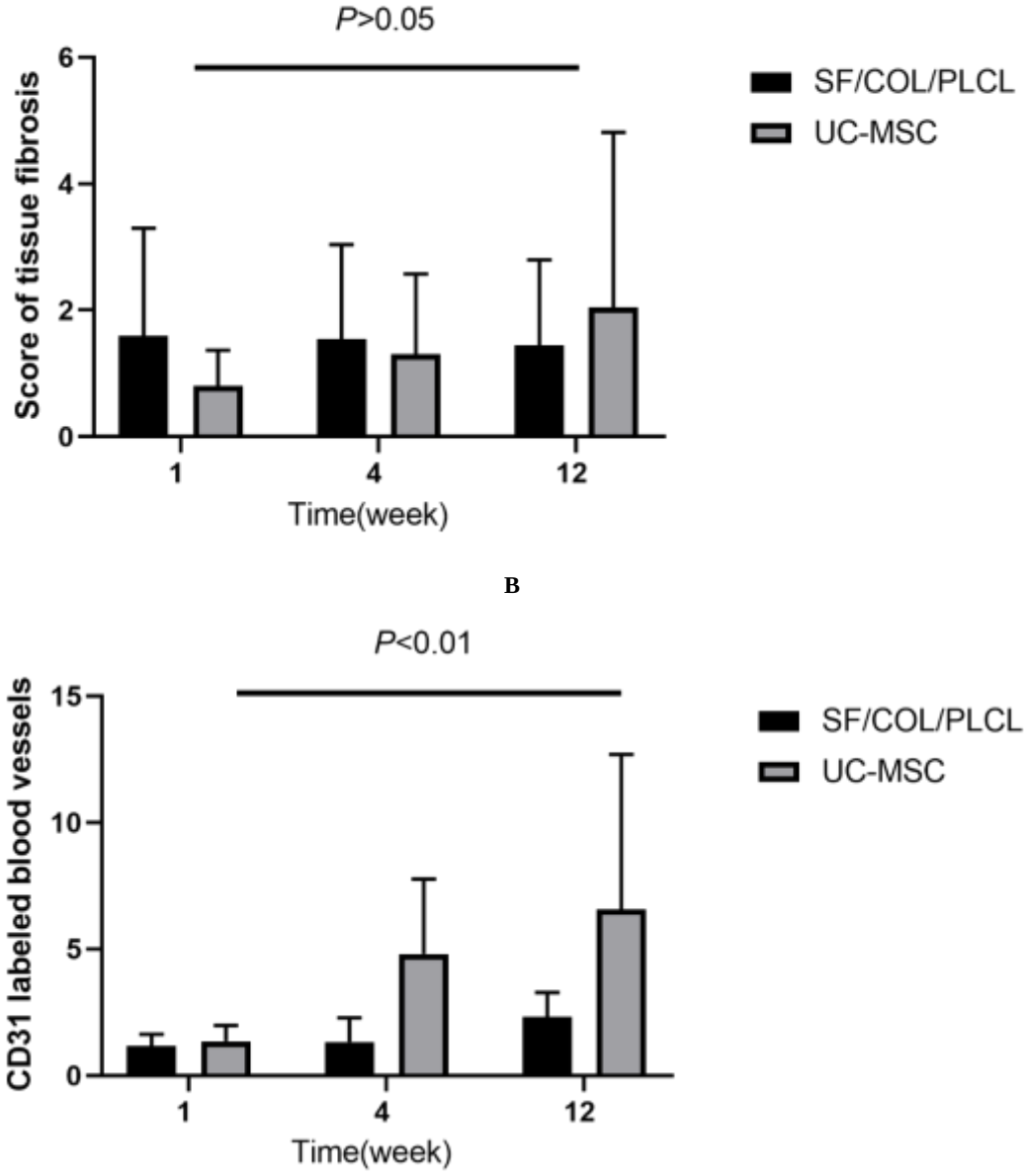

Figure 4: *The semi-quantitative pathohistological assessment of the control and umbilical cord-derived mesenchymal stem cell (UC-MSC)-seeded silk fibroin/collagen/poly(lactide-co-caprolactone) (SF/COL/PLCL) scaffold slides at different time points post-implantation. A, Inflammatory cell proliferation (F=23.79, p<0.01). B,Fibrosis score (F=2.40, p>0.05). C, Numbers of new blood vessels (F=81.75, p<0.01).*

The Masson and immunohistochemistry staining revealed that the UC-MSC-seeded scaffold group exhibited enhanced integration into rat tissues; the scaffolds had been completely degraded and they had been replaced by soft tissues, with evidence of extensive angiogenesis, based on the presence of CD-31-labelled blood vessels. The naked SF/COL/PLCL group had integrated poorly into the rat tissue, and the scaffold could still be seen by week 12. Comparing the naked SF/COL/PLCL nano-fibrous membrane with the UCMSC seeded nano-fibrous membrane, it was clear that the seeded scaffold exhibited significantly more CD-31-labelled blood vessels (F=81.75, $p<0.01$), but the tissue fibration score, between the two groups, had lower statistical significance (F=2.40, $p>0.05$; Figure 2, 3).

4.4. IL-2, IL-6, IL-8 and TNF-α levels tested by qRT-PCR

The relative levels of *IL-2*, *IL-6*, *IL-8*, and *TNF-α* in the surrounding tissue of the implant scaffold showed a general decreasing trend as time passed. Compared to the control SF/COL/PLCL scaffold, the UC-MSC-seeded scaffold had mildly elevated levels of *IL-6*, *IL-8*, and *TNF-α* in the surrounding tissue at 1 and 4 weeks post-implantation. There was no significant difference in the expression levels of *IL-2*, *IL-8*, and *TNF-α* between the two groups at each time point ($p>0.05$). However, the difference in *IL-6* levels between groups was statistically significant ($p<0.05$), and it was more obvious at 12 weeks ($P<0.01$; Figure 5).

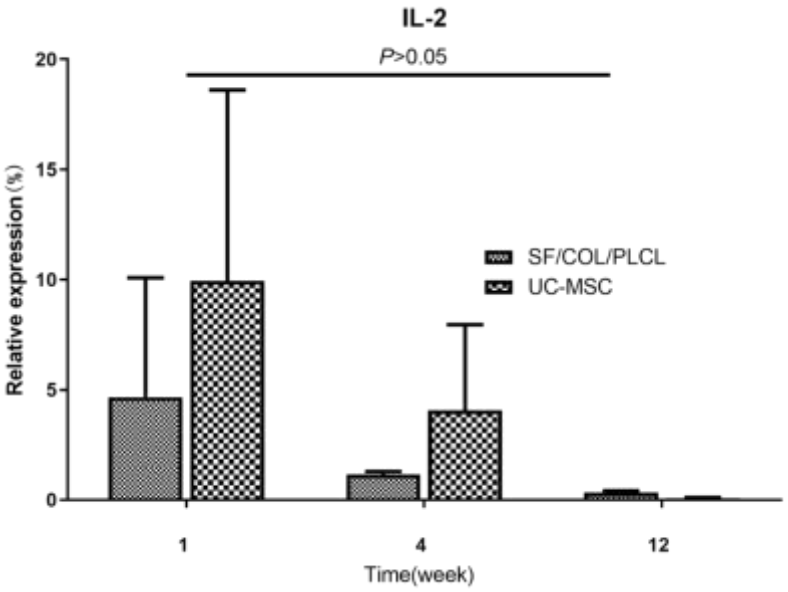
IL-2
P>0.05
Relative expression (%)
20
15
10
5
0
SF/COL/PLCL
UC-MSC
1
4
12
Time(week)

A

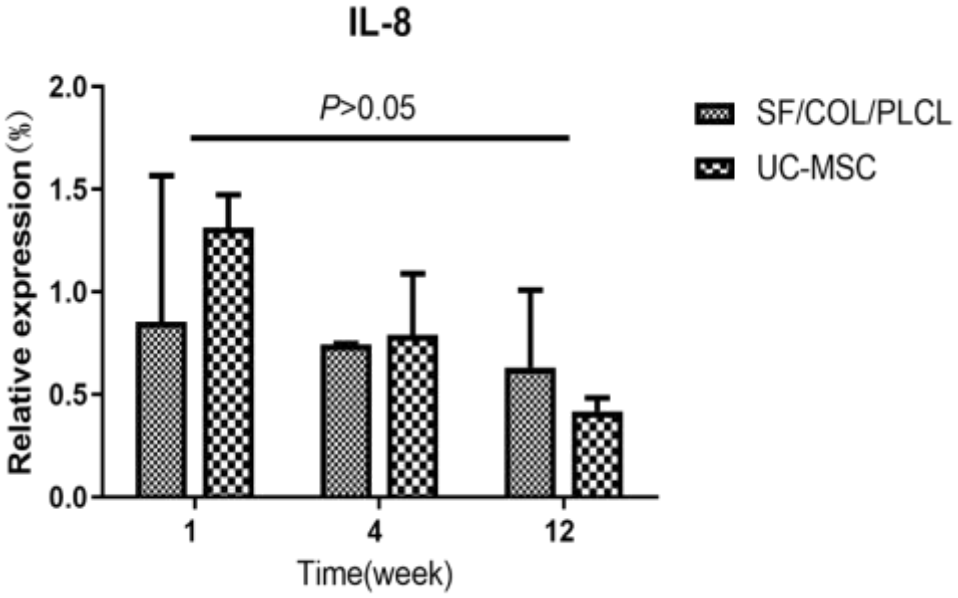
IL-8
P>0.05
Relative expression (%)
2.0
1.5
1.0
0.5
0.0
SF/COL/PLCL
UC-MSC
1
4
12
Time(week)

B

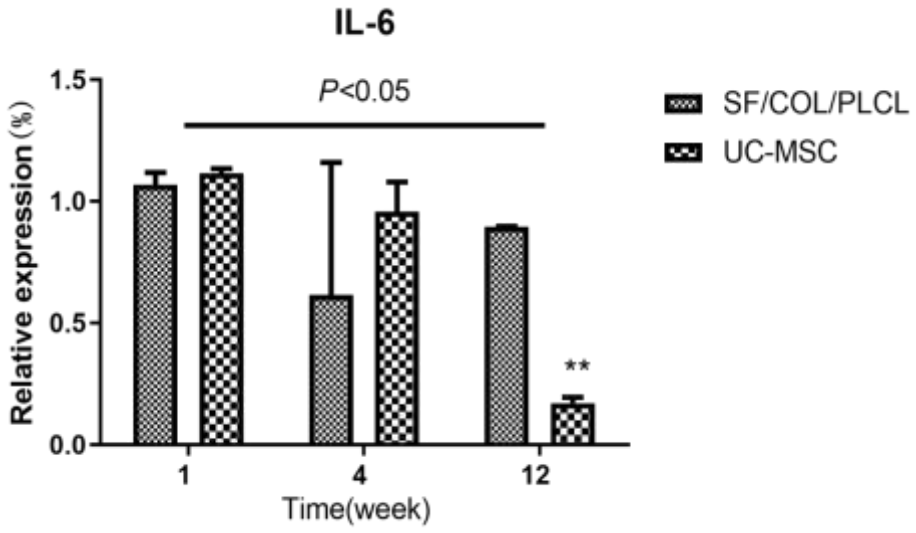

C

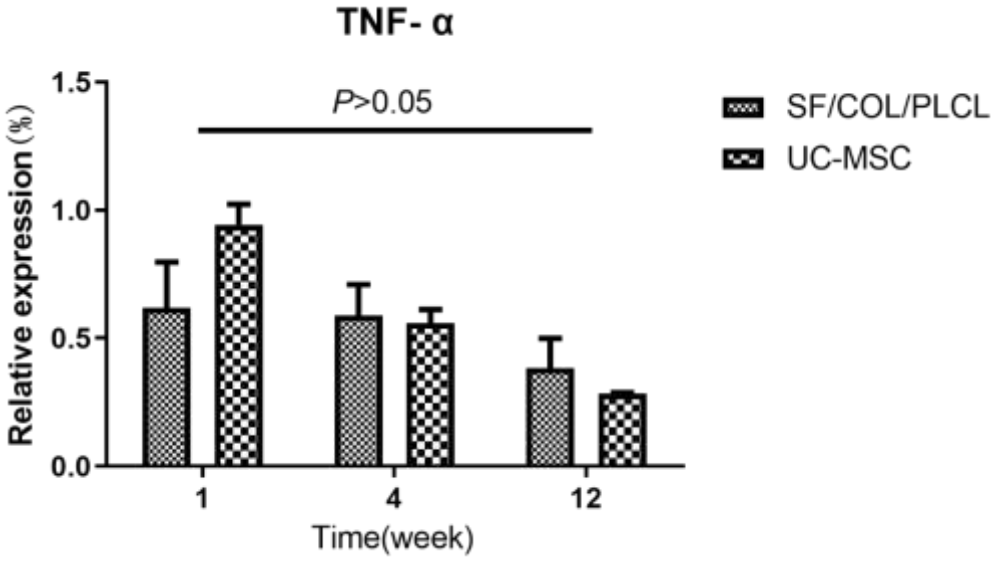

D

Figure 5: *The relative expression levels of inflammatory cytokines at different time points post- implantation. The difference in IL-2, IL-8, and TNF-α expression was not statistically significant (F values were 2.05, 2.00, and 7.21, respectively, p>0.05). The difference in IL-6 levels between groups was statistically significant (F value was 19.35, P<0.05), and was more obvious at 12 weeks (W) (P<0.01). A, IL-2, B, IL-6, C, IL-8, D,TNF-α, *P<0.05, ** P<0.01.*

5. Discussion

This study demonstrated that UC-MSCs grew well after inoculation onto nanofibrous scaffolds *in vitro*, and that cell numbers reached their maximum after 7 days. The cell morphology and extension were normal, indicating that the SF/COL/PLCL electrospun nanofibre scaffold was cell compatible.

When biomaterials are implanted in the body, they often trigger an inflammatory response immediately. An excessive inflammatory response not only leads to local tissue swelling and necrosis but also causes extensive fibrosis. When this occurs in the case of pelvic floor reconstruction, the implanted mesh often deforms and shrinks, resulting in increased stiffness in the local tissue. Our results showed that the SF/COL/PLCL patches seeded with UC-MSCs had a better histological score than the naked patch, despite an increase in infiltration by inflammatory cells in the tissue after 1 week. The improvement is more than likely facilitated by the rapid degradation of the implanted mesh, since we observed that by the end of the 12th week of study, the implanted patches seeded with UC-MSCs had completely degraded. This observation, along with the increase in the number of collagen fibres and evidence of extensive neovascularization, led us to speculate that this type of implanted mesh will be beneficial for patients suffering from POP.

This was further evidenced by the observed increases in the levels of inflammatory cytokines IL-6, IL-8, and TNF-α in the early stages post-implantation, which is suggestive of more extensive infiltration by

inflammatory cells, potentially induced by the enhanced degradation process, and the resulting absorption of the matrix by the host [23].

The inflammatory response to the seeded nanofibres ended up being a short-term response. By the end of the study, the levels of inflammatory cytokines were lower, suggesting more extensive inflammation resolution. This might be due to the documented [24] immunosuppressive properties of UC-MSCs, which have been attributed to their ability to suppress lymphocyte proliferation [25], along with enhanced degradation of the mesh.

IL-6 is a multifunctional cytokine, and multiple studies [26,28] have shown that IL-6 can directly stimulate angiogenesis, induce sprouting of isolated blood vessels, and impact cell proliferation, but the timing of inflammation is critical for these beneficial effects. Like the response to VEGF, continuous exposure to elevated levels of IL-6 can significantly impede the growth of blood vessels [29]. The fact that there were higher levels of IL-6 early on, but that levels dropped as the study progressed implies that the early inflammatory cytokine response, which ended up being beneficial, effectively promoted angiogenesis [30].

6. Conclusion

The SF/COL/PLCL patch seeded with UC-MSCs showed enhanced biocompatibility, resulting in a high degree of tissue fusion and reduced inflammation following implantation in rats. This research establishes a theoretical foundation for applying composite mesh structures to human pelvic floor reconstruction.

7. Acknowledgments

The authors would like to thank the nurses, clinicians, and management staff of Jinhua Maternal & Child Health Care Hospital. Thanks to Jinhua Food and Drug Inspection and Testing Institute for providing us with animal feeding and model making. Thanks to Jinhua Sdam Stem Cell Biotechnology Co., Ltd. for providing us with stem cells. for their participation in and support for this research.

8. Abbreviations

SF/COL/PLCL - Silk fibroin/collagen/poly(lactide-co-caprolactone)

UC-MSCs - Human umbilical cord-derived mesenchymal stem cells

FPFD - Female pelvic floor dysfunction

POP - Pelvic organ prolapse

9. Compliance with ethical standards

Conflict of interest: The authors declare that they have no conflict of interest.

10. Funding

This study was supported by the Basic Public Welfare Research Program of Zhejiang Province (LGF19H040001).

References

1. Chang Y, Sun X, Li Q. (2017). Silk fibroin scaffold as a potential choice for female pelvic reconstruction: A study on the biocompatibility in abdominal wall, pelvic, and vagina. Microscopy Research and Technique, 80, 291–297.
2. Weintraub A.Y, Glinter H, Marcus-Braun N. (2020). Narrative review of the epidemiology, diagnosis and pathophysiology of pelvic organ prolapse, International braz j urol: official journal of the Brazilian Society of Urology 46, 5-14.
3. Shafaat S, Mangir N, Regureos SR. (2018). Demonstration of improved tissue integration and angiogenesis with an elastic, estradiol releasing polyurethane material designed for use in pelvic floor repair, Neuro-urology and urodynamics 37, 716-725.
4. Dällenbach P. (2015). To mesh or not to mesh: a review of pelvic organ reconstructive surgery, International journal of women's health 7, 331-343.
5. Lo TS, Yusoff F.M, Kao C.C (2017). A 52-month follow-up on the transvaginal mesh surgery in vaginal cuff eversion, Taiwanese journal of obstetrics & gynecology 56, 346-352.
6. Haylen B.T, Sand P.K, Swift S.E. (2012). Transvaginal placement of surgical mesh for pelvic organ prolapse: more FDA concerns--positive reactions are possible, International urogynecology journal 23, 11-13.
7. Kasyan G, Abramyan K, Popov A.A. (2014). Mesh-related and intraoperative complications of pelvic organ prolapse repair, Central Europeanjournal of urology 67, 296-301.
8. Raya-Rivera A, Esquiliano D.R, Yoo J.J. (2011). Tissue-engineered autologous urethras for patients who need reconstruction: an observational study, Lancet (London, England) 377, 1175-1182.
9. Cheng J, Zhao Z.W, Wen J.R. (2020). Status, challenges, and future prospects of stem cell therapy in pelvic floor disorders, World journal of clinical cases 8, 1400-1413.
10. Sima Y, Chen Y. (2020). MSC-based therapy in female pelvic floor disorders, Cell & bioscience 10, 104.
11. Ding J, Han Q, Deng Me. (2018). Induction of human umbilical cord mesenchymal stem cells into tissue-forming cells in a murine model: implications for pelvic floor reconstruction, Cell and tissue research 372, 535-547.
12. Unal S, Arslan S, Yilmaz BK. (2020). Polycaprolactone/Gelatin/Hyaluronic Acid Electrospun Scaffolds to Mimic Glioblastoma Extracellular Ma trix Materials (Basel) 13(11):2661.
13. Wang Z, Hu J, Yu J. (2020). Preparation and Characterization of Nano-Laponite/PLGA Composite Scaffolds for Urethra Tissue Engineering, Molecular biotechnology 62, 192-199.
14. Zhang X.Y, Chen Y.P, Han J. (2019). Biocompatiable silk fibroin/carboxymethyl chitosan/strontium substituted hydroxyapatite/cellulose nanocrystal composite scaffolds for bone tissue engineering, International journal of biological macromolecules 136, 1247-1257.
15. Chen B.Q, Kankala R.K, Chen A.Z. (2017). Investigationof silk fibroin nanoparticle-decorated poly (l-lactic acid) composite scaffolds for osteoblast growth and differentiation, International journal of nanomedicine 12, 1877-1890.
16. Sarazin P, Roy X, Favis B.D. (2004). Controlledpreparationand properties of porous poly(L-lactide) obtained from a co-continuous blend of two biodegradable polymers, Biomaterials 25, 5965-5978.
17. Neuss S, Denecke B, Gan L. (2011). Transcriptome analysis of MSC and MSC-derived osteoblasts on Resomer® LT706 and PCL: impact of biomaterial substrate on osteogenic differentiation, PloS one 6, e23195
18. Mukherjee S, Darzi S, Rosamilia A. (2019). Blended Nanostructured Degradable Mesh with Endometrial Mesenchymal Stem Cells Promotes Tissue Integration and Anti-Inflammatory Response in Vivo for Pelvic Floor Application, Biomacromolecules 20, 454-468.
19. Noh Y.K, Du P, Kim I.G (2016). Polymer mesh scaffold combined with cell-derived ECM for osteogenesis of human mesenchymal stem cells, Biomater Res 20, 6.
20. Wu L.L, Pan X.M, Chen H.H. (2020). Repairing and analgesic effectsofumbilical cord mesenchymal stem cell transplantation

in micewith spinal cord injury.BioMed Research International, 2020, 7650354.
21. Liu Qi, Zhang Z.R, Yin L.H . (2014). Study on properties of SF/COL/PLCL and SF/COL/PLLA electrospinning three-dimensional nanofiber scaffold materials. Functional Materials, 3, 3141-3144(in Chinese).
22. Huffaker R.K, Muir T.W, Rao A. (2008). Histologic response of porcine collagen-coated and uncoated polypropylene grafts in a rabbit vagina model. American Journal of Obstetrics and Gynecology, 198, 582.e581–587.
23. Deng M, Ding J, Ai F. (2020). Impact of human umbilical cord-derived stem cells (HUMSCs) on host responses to a synthetic polypropylene mesh for pelvic floor reconstruction in a rat model. Cell and Tissue Research, 382, 519–527.
24. Weiss M.L, Anderson C, Medicetty S. (2008). Immune properties of human umbilical cord Wharton's jelly-derived cells. Stem Cells, 26, 2865–2874.
25. Schmidt-Bleek K, Schell H, Lienau J. (2014). Initial immune reaction and angiogenesis in bone healing. Journal of Tissue Engineering and Regenerative Medicine, 8, 120–130.
26. Autenshlyus A.I, Arkhipov S.A, Kunts T.A. (2017). Cytokine profiles of tumor supernatants in invasive ductal cancer and fibroadenoma of the breast and its relationship with VEGF-A expression in the tumors. International Journal of Immunopathology and Pharmacology, 30, 83–88.
27. Gopinathan G, Milagre C, Pearce O.M. (2015). Interleukin-6 Stimulates Defective Angiogenesis. Cancer Research, 75, 3098–3107.
28. Incio J, Ligibel J.A, McManus D.T. (2018). Obesity promotes resistance to anti-VEGF therapy in breast cancer by up-regulating IL-6 and potential ly FGF-2. Science Translational Medicine, 10, eaag0945.
29. Eichten A, Su. J, Adler A.P. (2016). Resistance to Anti-VEGF Therapy Mediated by Autocrine IL6/STAT3 Signaling and Overcome by IL6 Blockade. Cancer Research, 76, 2327–2339.
30. Schmidt-Bleek K, Schell H, Lienau J. (2014). Initial immune reaction and angiogenesis in bone healing. Journal of Tissue Engineering and Regenerative Medicine, 8, 120–130.

DOI: 10.31579/2767-7370/028

How to cite this Article: Jin Keqin, Luo Jianfeng, Su Aifang, Ding Mingxing, Fu Saihong, et al. (2022). Biocompatibility of MSC-Seeded Pelvic Patch. *J New Medical Innovations and Research,* 3(1);

DOI:10.31579/2767-7370/028